Role of Domain 4 in Sodium Channel Slow Inactivation

Nenad Mitrovic,*‡ Alfred L. George, Jr.,§‖ and Richard Horn*

From the *Department of Physiology, Jefferson Medical College, Philadelphia, Pennsylvania 19107; ‡Department of Applied Physiology and Neurology, University of Ulm, 89081 Ulm, Germany; and §Department of Medicine and ‖Department of Pharmacology, Vanderbilt University School of Medicine, Nashville, Tennessee 37232-6304

abstract Depolarization of sodium channels initiates at least three gating pathways: activation, fast inactivation, and slow inactivation. Little is known about the voltage sensors for slow inactivation, a process believed to be separate from fast inactivation. Covalent modification of a cysteine substituted for the third arginine (R1454) in the S4 segment of the fourth domain (R3C) with negatively charged methanethiosulfonate-ethylsulfonate (MTSES) or with positively charged methanethiosulfonate-ethyltrimethylammonium (MTSET) produces a marked slowing of the rate of fast inactivation. However, only MTSES modification produces substantial effects on the kinetics of slow inactivation. Rapid trains of depolarizations (2–20 Hz) cause a reduction of the peak current of mutant channels modified by MTSES, an effect not observed for wild-type or unmodified R3C channels, or for mutant channels modified by MTSET. The data suggest that MTSES modification of R3C enhances entry into a slow-inactivated state, and also that the effects on slow inactivation are independent of alterations of either activation or fast inactivation. This effect of MTSES is observed only for cysteine mutants within the middle of this S4 segment, and the data support a helical secondary structure of S4 in this region. Mutation of R1454 to the negatively charged residues aspartate or glutamate cannot reproduce the effects of MTSES modification, indicating that charge alone cannot account for these results. A long-chained derivative of MTSES has similar effects as MTSES, and can produce these effects on a residue that does not show use-dependent current reduction after modification by MTSES, suggesting that the sulfonate moiety can reach a critical site affecting slow inactivation. The effects of MTSES on R3C are partially counteracted by a point mutation (W408A) that inhibits slow inactivation. Our data suggest that a region near the midpoint of the S4 segment of domain 4 plays an important role in slow inactivation.

key words: thiol reagents • cysteine modification • S4 segment • site-directed mutagenesis

INTRODUCTION

The hallmark of sodium channel function is its transient nature, which is due primarily to the coordinated interplay between two rapid kinetic processes, activation and fast inactivation. These processes are initiated within a few milliseconds after voltage sensors of the channel move in response to a depolarization. Another contributor to sodium channel function, slow inactivation, takes place on a time scale of seconds to minutes. Excitability of muscle and nerve cells requires a delicate balance between these three gating processes; defects in any of them can result in potentially fatal pathologies (Ji et al., 1995; Barchi, 1995; Cannon, 1996; Lehmann-Horn and Jurkat-Rott, 1999).

Of the above gating mechanisms, activation and fast inactivation have been examined most extensively. We know, for example, that the main voltage sensors for activation of voltage-gated ion channels are the four positively charged S4 segments, one within each homologous domain of sodium or calcium channels, or within each subunit of potassium channels (Catterall, 1986; Keynes, 1994; Sigworth, 1994; Yellen, 1998; Keynes and Elinder, 1999; Bezanilla, 2000). The activation gates of potassium channels are believed to be at the cytoplasmic end of the four S6 segments (Holmgren et al., 1997; Liu et al., 1997). In sodium channels, the cytoplasmic loop between domains 3 and 4 may act as the fast-inactivation gate, closing the permeation pathway in a "hinged-lid" fashion in response to a depolarization (West et al., 1992). Most of the voltage dependence of fast inactivation comes from coupling to activation (Armstrong, 1981; French and Horn, 1983; Patlak, 1991; Keynes, 1994; Goldman, 1999; Keynes and Elinder, 1999).

The S4 segment of the fourth homologous domain in sodium channels (D4/S4)[1] is likely to be involved in this coupling, because mutations in D4/S4 have large effects on rates of both inactivation (Chahine et al., 1994; Chen et al., 1996; Kontis and Goldin, 1997) and deactivation (Ji et al., 1996; Groome et al., 1999). Furthermore, conformational changes measured with fluorophores inserted near D4/S4 have kinetics similar to those of fast inactivation (Cha et al., 1999).

Address correspondence to Dick Horn, Department of Physiology, Jefferson Medical College, 1020 Locust St., Philadelphia, PA 19107. Fax: 215-503-2073; E-mail: richard.horn@mail.tju.edu

[1]*Abbreviations used in this paper:* D4/S4, the S4 segment of the fourth homologous domain; MTSET, methanethiosulfonate-ethyltrimethylammonium; MTSES, methanethiosulfonate-ethylsulfonate; MTSPeS, methanethiosulfonate-pentylsulfonate; S_{∞}, steady state slow inactivation.

J. Gen. Physiol. © The Rockefeller University Press • 0022-1295/2000/06/707/11 $5.00
Volume 115 June 2000 707–717
http://www.jgp.org/cgi/content/full/115/6/707

Much less is known about slow inactivation. Recent studies suggest that fast and slow inactivation are distinct processes, but it is not clear whether they are independent or coupled to each other in some way (Featherstone et al., 1996; Nuss et al., 1996; Vedantham and Cannon, 1998). The locations of the slow inactivation gate and its voltage sensors are also unknown. However, mutations in S5 and S6 segments, and also in cytoplasmic S4–S5 linkers, can affect slow inactivation (Cummins and Sigworth, 1996; Hayward et al., 1997, 1999; Wang and Wang, 1997; Bendahhou et al., 1999; Takahashi and Cannon, 1999). Furthermore, there is evidence that the extracellular entrance to the permeation pathway plays a role in slow inactivation (Balser et al., 1996; Townsend and Horn, 1997; Todt et al., 1999; Vilin et al., 1999). A mutation in D2/S4 also affects slow inactivation (Fleig et al., 1994), suggesting that this transmembrane segment may contribute to the voltage dependence of slow inactivation.

Here we report that chemical modification of cysteines substituted for residues in D4/S4 causes pronounced changes in slow inactivation, suggesting that D4/S4 and the transmembrane segments surrounding it play important roles in the voltage dependence of slow inactivation.

MATERIALS AND METHODS

Mutagenesis

The cysteine mutations in the S4 segment of domain 4 were constructed in the human skeletal muscle sodium channel hSkM1, as described previously (Chahine et al., 1994; Yang et al., 1996, 1997). We denote the point mutants as follows. The outermost charged residue, arginine 1448 is called R1, and its cysteine substitute is called R1C. The other seven basic residues when substituted individually by cysteine, are denoted as R2C, R3C, R4C, R5C, R6C, K7C (a lysine in the wild-type channel), and R8C. Other cysteine mutants in D4/S4 are denoted by the residue number. For example, the cysteine substitution for a leucine residue at position 1452 is denoted L1452C.

Mutations R3E and R3D at position 1454 and two additional D4/S4 cysteine mutants (I1455C, G1456C) were constructed similarly to R3C as described by Yang et al. (1996), using the following antisense mutagenic primers: R3E: 5′-ATG CCC TTG GCC CCG CGG ATC AGC CGC AGG ACG CGT CCA ATC TCC GCC AGG CGG ATC ACA CGG AAC -3′; R3D: 5′'-ATG CCC TTG GCC CCG CGG ATC AGC CGC AGG ACA CGC CCG ATA TCC GCC AGG CGG ATC ACA CGG AAC-3′; L1455C: 5′-ATG CCC TTG GCC CCG CGG ATC AGC CGC AGG ACA CGG CCG CAC CGC GCC AGG CGG ATC ACA; and G1456C: 5′-ATG CCC TTG GCC CCG CGG ATC AGC CGC AGt ACt CGa CaA ATC CGC GCC AGG CGG ATC A-3′. Mutant fragments generated by the polymerase chain reaction were subcloned into pRc/CMV-hSkM1 and sequenced to exclude polymerase errors and to verify the mutation.

To make the point mutation W408A (equivalent to W402A in the rat skeletal muscle sodium channel), we used a recombinant polymerase chain reaction strategy (double-overlap method; Higuchi, 1989). The mutagenic primer (5′-CTC ATG ACA CAG GAC TAT **GC**G GAG AAC CTC TTC CAG CTG ACC CT**G** CG**C** GCA GCT GGC AAG ACC TAC-3′) spanning nucleotides 1204–1275 (numbering relative to the open reading frame) and its inverse complement were used in conjunction with two flanking primers (forward: 5′- TCA TCC CAG GGC TGA AGA C-3′; reverse: 5′-AGC ATC TGC TGA AAC TC-3′) to create the mutation (changed codon underlined) and incorporate a silent BssHII site (for use in clone screening) in the final 721-bp product. Amplifications were performed using 20 ng of hSkM1-SA cDNA (containing a silent HindIII site at position 1302) (Makita et al., 1996) as template and Expand™ DNA polymerase (Roche Molecular Biochemicals). Final products were purified by spin-column chromatography (Qiagen), digested with SapI and HinDIII, and the resulting 485-bp fragment assembled into the full-length plasmid pRc/CMV-hSkM1. The amplified region was sequenced entirely in the final construct to verify the mutation and to exclude polymerase errors.

The double mutant W408A/R3C was created by ligating a 2.8-kb NotI/XhoI fragment from W408A with a 3.3-kb XhoI/XbaI fragment from hSkM1 mutation R1454C (R3C) into the pRc/CMV vector. Sequencing was used to verify assembly and the presence of both mutations.

Electrophysiology and Data Acquisition

Standard whole-cell recording methods were used as previously described (Yang and Horn, 1995), after heterologous transient expression in tsA201 cells, a transformed variant of HEK293 cells. Supercharging reduced the expected charging time constant for the cells to <10 μs. Series resistance errors were <3 mV after correction by the patch-clamp amplifier, an Axopatch 200A (Axon Instruments, Inc.). Data were acquired using pCLAMP (Axon Instruments, Inc.), and except where indicated, were filtered at 5 kHz. Patch electrodes contained (mM): 105 CsF, 35 NaCl, 10 EGTA, 10 HEPES, titrated to pH 7.4 with CsOH. The bath contained (mM): 150 NaCl, 2 KCl, 1.5 $CaCl_2$, 1 $MgCl_2$, 10 HEPES, titrated to pH 7.4 with CsOH. Corrections were made for liquid junction potentials. Except where indicated, the experiments were done at room temperature (20–22°C). For tail currents, the temperature was set at 12.0 ± 0.1°C by use of feedback-regulated Peltier devices (Dagan Corp.) and data were low-pass filtered at 10 kHz.

Methanethiosulfonate-ethyltrimethylammonium (MTSET), -ethylsulfonate (MTSES), and -pentylsulfonate (MTSPeS), were obtained from Toronto Research Chemicals. MTSET covalently attaches ethyltrimethylammonium to the reduced cysteine sulfhydryl via a disulfide bond, MTSES attaches ethylsulfonate, and MTSPeS attaches pentylsulfonate. Aqueous stocks of these reagents were kept at 4°C, and diluted in the bath solution immediately before use. The reagent solutions were presented with a macropipette placed in apposition to the cell (Yang et al., 1997). Typically, 100 μM MTSET, 5 mM MTSES, and 1–5 mM MTSPeS were applied under depolarizing conditions until the channels were completely modified, as indicated by effects on the inactivation kinetics (Yang et al., 1997). In some experiments, the reagents were applied to a dish of cells for 10 min before washing the dish with the bath solution. For residues accessible only internally, the reagent was placed in the patch pipette at the above concentrations (Yang et al., 1996, 1997).

Data Analysis

Whole-cell data were displayed and analyzed by a combination of pCLAMP programs, Excel (Microsoft), ORIGIN (MicroCal), and our own FORTRAN programs. Data from at least three cells for each measurement are presented as mean ± SEM. We fit data from individual cells to theoretical functions of choice, and the reported values are the means and standard errors of the estimated parameters from these individual fits.

Steady-state slow inactivation (S_∞) was measured at −20 mV us-

ing 60-s conditioning pulses followed by a 50- or 100-ms prepulse at −120 mV to remove fast inactivation. There was no difference between these durations of prepulse. Boltzmann functions were fit to the S_∞ data by use of the Levenberg-Marquardt algorithm in Origin. The midpoint ($V_{0.5}$) and slope (q, the valence in units of the number of elementary charges) were estimated from fits to individual cells. Although the fit of data for each cell to a Boltzmann function was excellent, there was considerable cell-to-cell variability in the fraction of available channels after conditioning pulses to positive membrane potentials [the ranges of $S_\infty(V+)$ are given in the legend to Fig. 4]. This distorted the shape of the S_∞ relationship when we averaged data from different cells. To obviate this problem, we scaled the data from each cell between the maximum inward current (set at 1.0) and the mean value of $S_\infty(V+)$ for all cells. The scaling of $S_\infty(V+)$ was made according to the best-fit theoretical function for an individual cell. This procedure allowed us to plot the mean ± SEM of the normalized data (see Fig. 4), which were well described by the expected Boltzmann function generated from the means of the parameters from fits to individual cells.

RESULTS

Mutations of residues in D4/S4 affect both the kinetics and the steady state values of fast inactivation (Chahine et al., 1994; Chen et al., 1996; Kontis and Goldin, 1997; Kühn and Greeff, 1999; Sheets et al., 1999). Similarly, covalent modification of cysteines substituted for D4/S4 residues affects these characteristics of fast inactivation (Yang and Horn, 1995; Yang et al., 1996, 1997). Examples are shown in Fig. 1 for cysteine mutants of the first and third positively charged arginines in D4/S4 of the human skeletal muscle sodium channel (R1C and R3C). Whole-cell currents were obtained from transfected tsA201 cells. The sodium currents in Fig. 1 were elicited by a series of depolarizing pulses from a −140-mV holding potential, starting from −90 mV, in 5-mV increments. The kinetics of the currents through wild-type channels (not shown) are similar to those of R3C channels (Yang et al., 1996). However, in accordance with previous reports (Chahine et al., 1994; Fan et al., 1996), the R1C mutant shows a slowing of the kinetics of fast inactivation and a reduction in its voltage dependence (Fig. 1).

The methanethiosulfonate reagents MTSET and MTSES alter the kinetics of inactivation of these two mutants, although in opposite directions (Fig. 1). Both reagents increase the inactivation rate of R1C, but decrease the inactivation rate of R3C. In both mutants, the cationic reagent MTSET, for reasons we do not understand, has a larger effect on these rates than the anionic reagent MTSES.

Use Dependence

While doing these experiments, we noticed that repetitive depolarizations of the R3C mutant, after modification by MTSES, caused a reduction of the peak inward current, even at rates as low as 1 Hz. Each panel in Fig. 2 shows 30 superimposed currents elicited by 9.6-ms depolarizations to −20 mV from a holding potential of

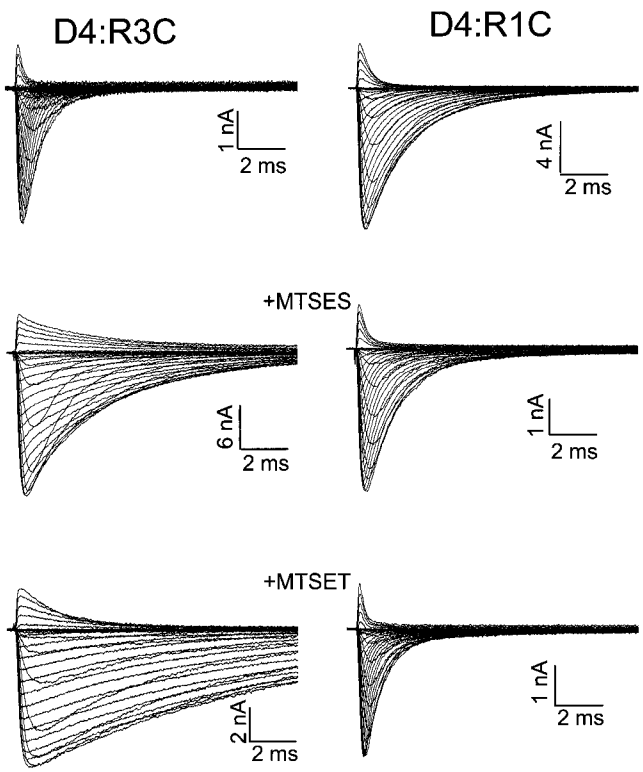

Figure 1. Effect of MTS reagents on R3C and R1C. Each panel shows the sodium currents from a different cell, unmodified and modified by either MTSET or MTSES. Currents were elicited by voltage steps (−90 to +65 mV in 5-mV increments) from a holding potential of −140 mV.

−150 mV at a frequency of 5 Hz. The effects of MTSET and MTSES on the kinetics of fast inactivation are consistent with the data of Fig. 1 for both R1C and R3C. The use-dependent reduction of sodium current is only observed for R3C modified by MTSES (R3C-SES). These data are not consistent with the possibility that the use dependence in R3C is a direct consequence of effects of MTSES on fast inactivation, because MTSET has a much larger effect on inactivation kinetics without producing this use dependence.

A similar use-dependent reduction of sodium currents is observed with local anesthetics (Strichartz, 1973). The local anesthetic effect is both frequency and voltage dependent. Fig. 3 shows that this is also the case for R3C-SES, using in all cases a holding potential of −150 mV. Unmodified R3C shows no use dependence for −20-mV depolarizations, even at stimulation rates up to 20 Hz (Fig. 3, top left). However, R3C-SES has a use dependence that increases in magnitude and rate with both increased stimulation rates and greater depolarizations.

Slow Inactivation

Superficially, these data suggest the possibility that MTSES modification of R3C enhances slow inactivation. For example, MTSES modification may increase

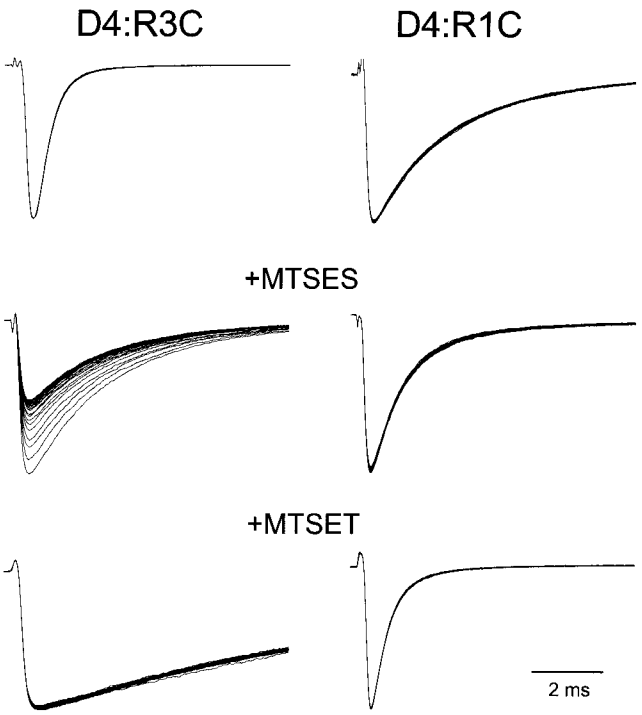

Figure 2. 5 Hz use dependence for R3C and R1C. Each panel shows 30 superimposed traces of currents generated by 9.6-ms depolarizations to −20 mV, presented at a rate of 5 Hz. A significant current reduction is seen only for R3C after modification by MTSES.

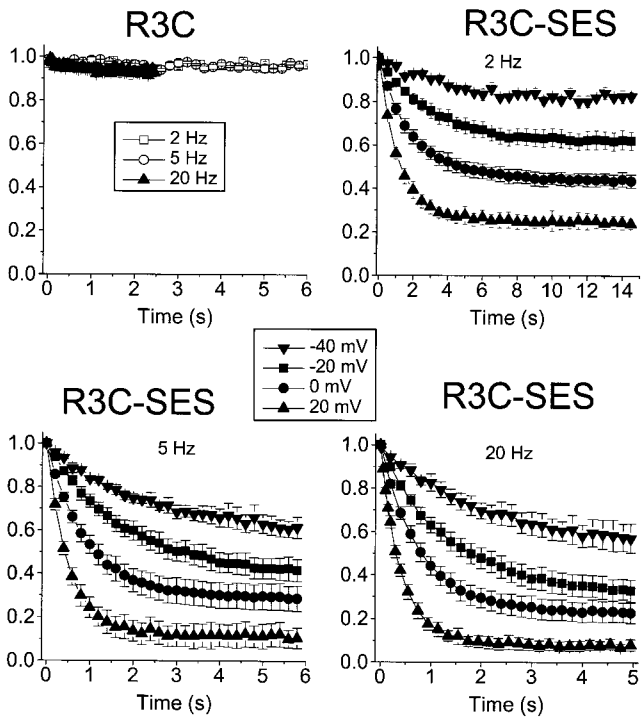

Figure 3. Frequency and voltage dependence of the use dependence of R3C. Each panel plots the mean ± SEM for normalized peak current for $n = 4$ or 5 cells. The holding potential was −150 mV in all cases. (Top left) Unmodified R3C shows no use-dependent current reduction for depolarizations to −20 mV at frequencies up to 20 Hz. The other three panels show data for R3C after modification by MTSES.

the rate of entry into a slow-inactivated state from which recovery is slow. To investigate this possibility, we examined the steady state and kinetic properties of slow inactivation in R3C mutants, either unmodified or modified by MTS reagents. Fig. 4 shows data for S_∞ obtained in response to 1-min conditioning pulses to the indicated voltages. Fast inactivation was recovered by a brief prepulse at −120 mV before the test pulse (see materials and methods). The data in each case were well fit by Boltzmann functions (Fig. 4, legend, and materials and methods). Both MTS reagents affect S_∞. MTSET causes a 12-mV depolarizing shift and a modest destabilization of slow inactivation at depolarized voltages. By contrast, MTSES causes a 28-mV hyperpolarizing shift of S_∞ and a stabilization of slow inactivation at depolarized voltages. These data suggest that MTSES either increases the rate of entry into, or decreases the rate of exit from, a slow-inactivated state.

The kinetics of slow inactivation were explored by the experiments shown in Fig. 5. We used the peak inward current for a brief depolarization as an assay of the available channels. For the experiments shown in Fig. 5 A, both fast and slow inactivation were caused by a 10-s depolarization to −40 mV. We measured the peak current at −20 mV as a function of the duration of a recovery interval at −150 mV. The normalized data were fit to sums of exponential relaxations (Fig. 5, legend). Note the logarithmic time base, as data were obtained over a range of more than four orders of magnitude.

Although the time course of recovery required three exponentials for a good fit in the cases of R3C and R3C after modification by MTSET (R3C-SET) (Fig. 5 A, legend), a single time constant of 2.91 ± 0.14 s was adequate for R3C-SES. The predominant time constant for recovery in R3C was 154 ± 16 ms, and for R3C-SET was 139 ± 21 ms. The data for R3C and R3C-SET are almost indistinguishable at this recovery voltage. As predicted, the recovery rate after a prolonged depolarization is markedly decreased by MTSES modification of R3C. Note that the recovery in this experiment includes both fast and slow inactivation.

The slowest time constants for recovery in Fig. 5 A were comparable (2.61, 2.09, and 2.91 s for R3C, R3C-SET, and R3C-SES, respectively). This could represent the time constant for recovery from slow inactivation at −150 mV in each case. This suggests that MTSES modification either inhibits recovery from fast inactivation or strongly enhances entry into a slow-inactivated state. Recovery time constants from fast inactivation are not, however, strongly inhibited by R3C-SES (data not shown), supporting the latter alternative.

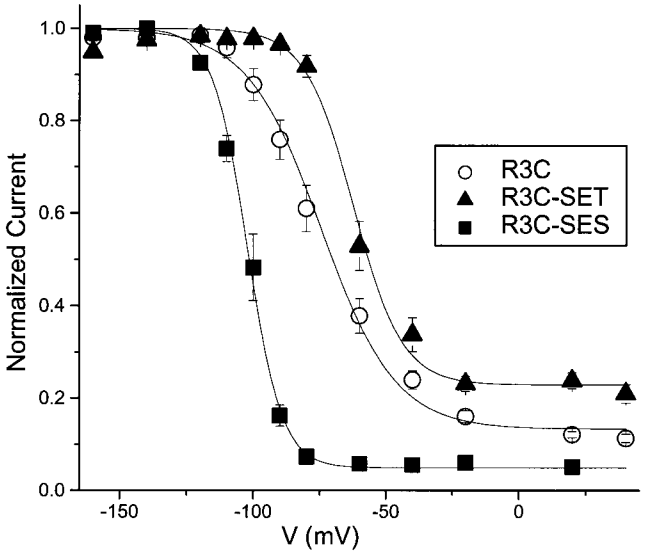

Figure 4. S-infinity. Steady state slow inactivation (S_∞) is plotted against conditioning voltage for n = 6–8 cells. The voltage protocol and method of analysis are described in materials and methods. The Boltzmann curves have midpoints and slopes of −74.4 ± 3.5 mV, 1.78 ± 0.10 e_0; −62.2 ± 2.5 mV, 2.72 ± 0.31 e_0; and −102.2 ± 1.4 mV, 3.82 ± 0.08 e_0 for R3C, R3C-SET, and R3C-SES, respectively. The range of fits for S_∞(V+) for R3C for individual cells was 0.051–0.245 (0.133 ± 0.020, n = 8); for R3C-SET it was 0.066–0.386 (0.229 ± 0.047, n = 6); for R3C-SES it was 0.003–0.085 (0.049 ± 0.014, n = 6).

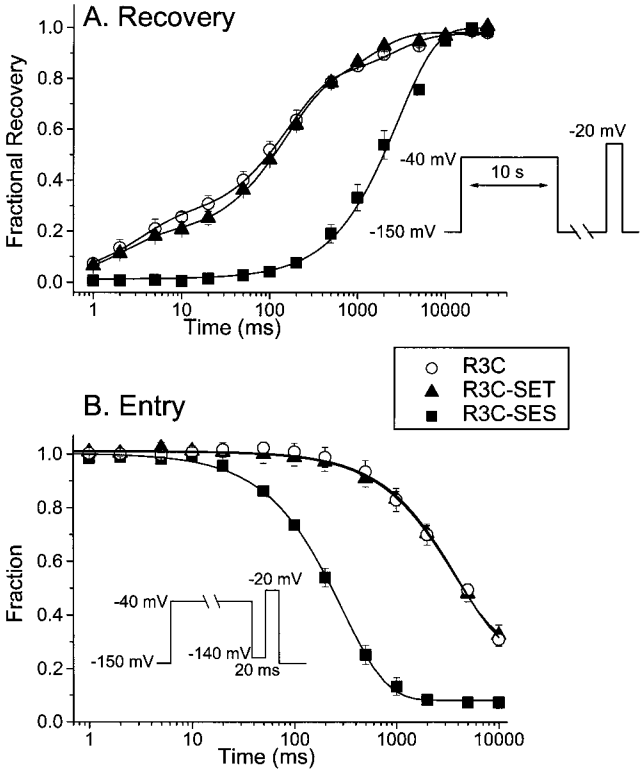

Figure 5. Kinetics of recovery from and entry into a slow inactivated state. Data from n = 3–4 cells for each condition. The voltage protocols are shown as insets. For recovery (A), one time constant (2.91 ± 0.14 s) fit the data well for R3C-SES. However, three time constants were needed for R3C (2.61 ± 0.73 s, 154 ± 16 ms, and 3.21 ± 0.91 ms) with fractional weights (0.20, 0.56, and 0.24), and for R3C-SET the time constants were 1.32 ± 0.39 s, 139 ± 21 ms, and 2.09 ± 1.04 ms, with fractional weights of 0.26, 0.55, and 0.19. Parameters for fits to the entry data (B) are given in the text.

To test this possibility, we measured the entry kinetics into a slow-inactivated state by the voltage protocol shown in Fig. 5 B. The entry voltage in this experiment was −40 mV. Fast inactivation was removed by a 20-ms prepulse to −140 mV before applying the test pulse at −20 mV. The normalized data in Fig. 5 B were fit in each case by a single exponential relaxation with time constants of 4.06 ± 0.34 s, 3.74 ± 0.14 s, and 299 ± 9 ms, respectively, for R3C, R3C-SET, and R3C-SES. Again, the data for R3C and R3C-SET are nearly indistinguishable in this experiment, but are dramatically different from those for R3C-SES. MTSES appears to increase the rate of entry into a slow-inactivated state.

It is somewhat surprising that R3C and R3C-SET are different in the steady state inactivation experiments of Fig. 4, but not in these kinetic experiments. We have no definitive explanation for this apparent discrepancy; however, it could be due to the limited voltages we examined in the kinetic experiments, recovery at −150 mV and entry at −40 mV, or to the longer conditioning pulse (60 s) used for studying steady state inactivation. An "ultra-slow" inactivation process may be accessed by such prolonged conditioning pulses (Todt et al., 1999).

Note that, although we can formally describe the action of MTSES on R3C as an effect on slow inactivation, we have not eliminated the possibility that it has a separate effect on the channel that is independent of the slow-inactivation process. This alternative will be considered below.

Dissection of D4/S4 for Effects on Use Dependence

Is the effect of MTSES on use dependence unique to the mutant R3C? To explore this, we tested the effects of MTSET and MTSES on cysteine mutants along the full length of D4/S4. Fig. 6 shows examples for two of these mutants, L1452C and A1453C, the two amino acids between R2 and R3 in the primary sequence. Use dependence was measured at 5 Hz from a holding potential of −150 mV, as in Fig. 2. Each panel in Fig. 6 shows 30 superimposed currents at −20 mV. These two cysteine residues are only accessible to intracellular reagents at hyperpolarized voltages (Yang et al., 1997). Therefore, the MTS reagents were added to the pipette solution during whole cell recording. Both MTSET and MTSES modification affected fast inactivation in both mutants. However, a use-dependent current reduction was only observed for A1453C after modification by

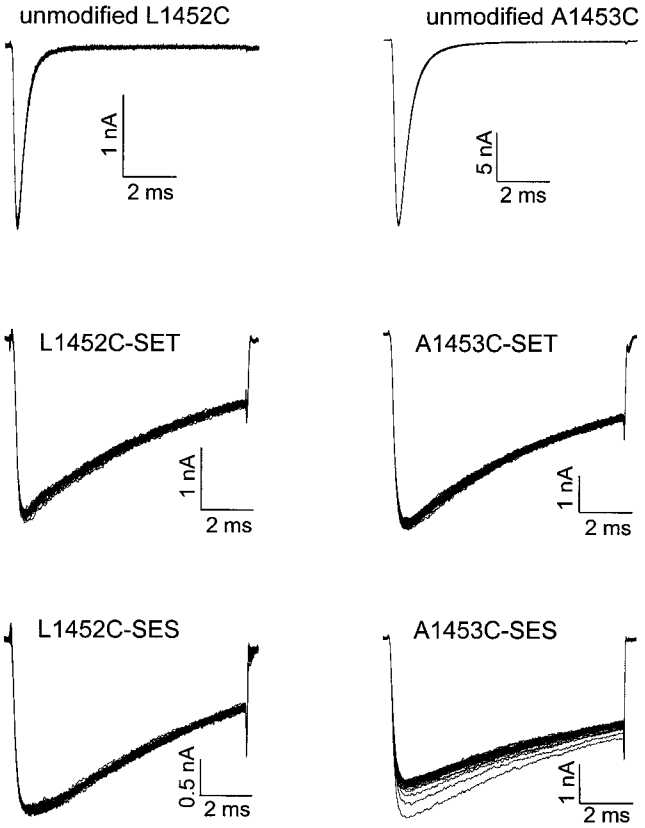

Figure 6. Test of 5 Hz use dependence for L1452C and A1453C. 30 superimposed currents shown in each panel for modified and unmodified mutant channels. Conditions identical to those in Fig. 2.

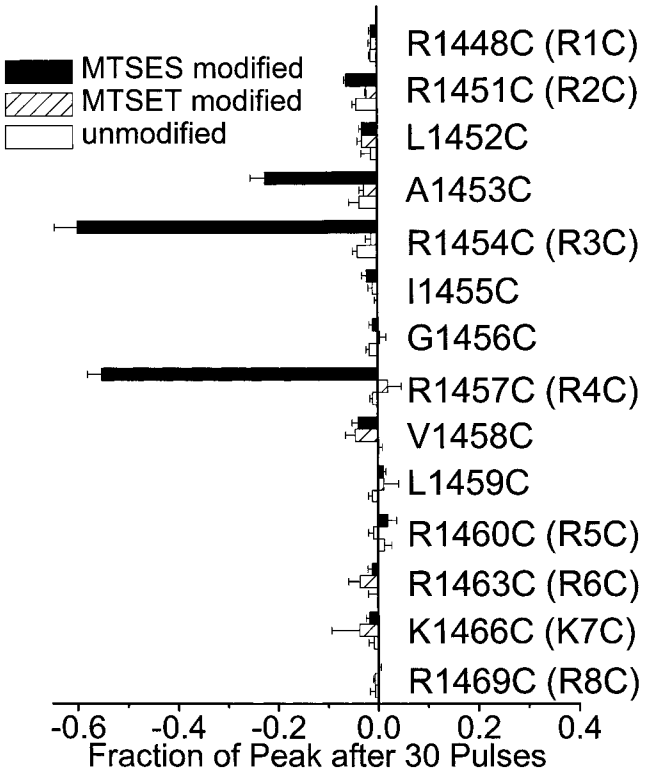

Figure 7. 5 Hz use dependence for 14 cysteine mutants in D4/S4. Mean ± SEM (n = 3–8) fractional current reduction for steps to −20 mV (9.6 ms from holding potential of −150 mV, 30 depolarizations).

MTSES. The effect was more modest than that observed for R3C modified by MTSES (Figs. 2 and 7).

The data for 14 cysteine mutants are summarized in Fig. 7, which plots the 5 Hz use dependence under the same conditions used in Figs. 2 and 6. Use-dependent current reduction is only observed after modification by MTSES, and this phenomenon is localized to the central region of D4/S4, between residues 1453 and 1457. The most pronounced current reduction is obtained with R3C and R4C.

It is notable that cysteine mutants of the isoleucine and glycine residues between R3 and R4, namely, I1455C and G1456C, do not exhibit a hint of use dependence after modification by MTSES (Figs. 7 and 8 A). Fig. 8 B shows that this pattern is consistent with an α helical secondary structure in this region of D4/S4, as if one face of the helix, encompassing R3, R4, and A1453, can affect slow inactivation. These data dovetail nicely into our previous evidence, based on cysteine accessibility, that the region between R2 and R3 has a helical secondary structure (Yang et al., 1997).

Role of Charge and Length of Tether in Use Dependence

The striking difference between the effects of MTSET and MTSES suggests that charge plays a role. S4 segments of sodium channels and most other voltage-dependent ion channels contain only neutral or positively charged residues. This raises the possibility that the hydrophobic region surrounding an S4 segment is "impermeable" to an anionic sidechain. Thus, the ethylsulfonate adduct of MTSES may restrict S4 movement through this region more than ethyltrimethylammonium, even though the anionic adduct is smaller. To test this idea, we mutated R1454 to either aspartate (R3D) or glutamate (R3E), both negatively charged, and looked for use-dependent current reduction. Residue 1454 was chosen because it showed the largest effect when mutated to cysteine and modified by MTSES (Fig. 7).

Although R3D and R3E both slow the rate of fast inactivation (Fig. 9, A and B, compare with unmodified R3C in Fig. 1), neither mutant produces a use-dependent current reduction at a stimulation rate of 5 Hz (Fig. 9, C and D). These results show that charge itself cannot be responsible for the different effects of modification by MTSET and MTSES.

These results raise the possibility that the S-ethylsulfonate adduct introduced by MTSES delivers its negative charge at an optimal distance from the S4 backbone to produce its effects on slow inactivation. To explore this idea, we tested a pentyl derivative of MTSES, MTSPeS, which extends the alkyl chain by three car-

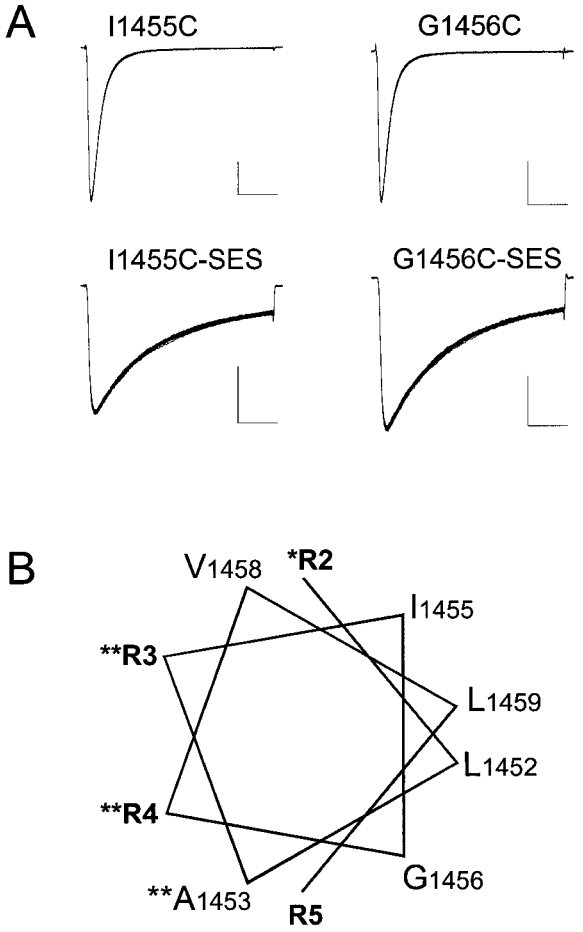

Figure 8. Lack of 5 Hz use dependence for I1455C and G1456C. A shows data for each mutant, either unmodified or modified by MTSES, using conditions and display identical to those in Fig. 2. The calibration bars represent 2 nA and 2 ms. B shows a helical wheel plot (100° angle between successive residues) between R2C and R5C, showing that significant use dependence is observed for modification along one face of the helix. *Use dependence only for MTSPeS. **Use dependence for both MTSES and MTSPeS.

bons. MTSPeS was used to modify the 10 cysteine mutants between R2 and R5, a region that brackets the residues that exhibit use-dependent current reduction when modified by MTSES. Fig. 10 shows that MTSPeS produces use dependence in the same three mutants (A1453C,[2] R3C, and R4C) that show use dependence after modification by MTSES. Moreover, it also causes use dependence in R2C, but not in the two residues between R2 and R3 in the primary sequence. This result is again consistent with a helical secondary structure in this part of D4/S4 (Fig. 8 B). The ability of the longer-chained derivative to produce this effect in R2C suggests that the long tether allows the sulfonate adduct to reach a site that affects slow inactivation (see discussion).

[2]The use-dependent current reduction is small for A1453C-SPeS, but significant (12.5 + 2.3%, $n = 3$). By comparison, the reduction is 22.5 + 2.9% ($n = 3$) for A1453C-SES (Fig. 7).

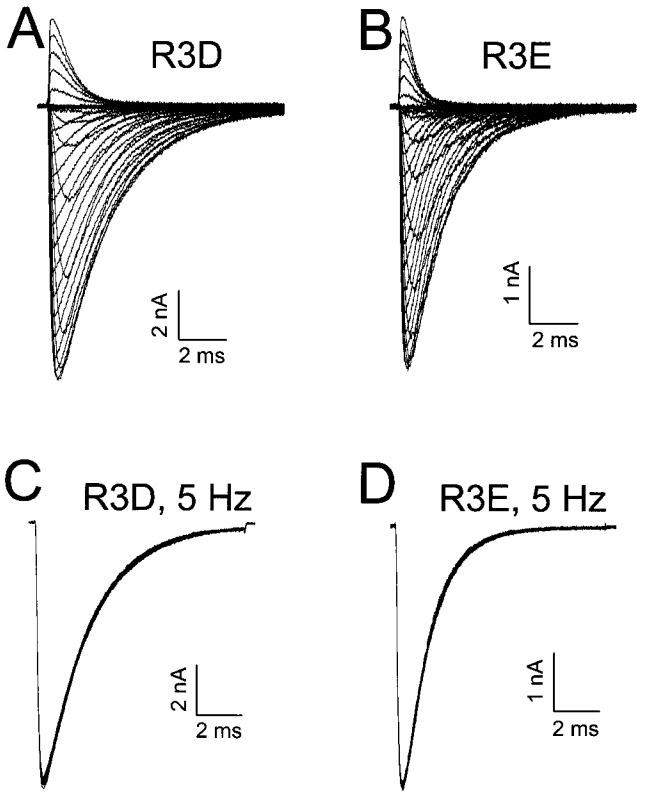

Figure 9. Charges and use dependence. The mutants R3D and R3E both affect the kinetics of fast inactivation (A and B), but neither causes use-dependent current reduction at 5 Hz stimulation rates (C and D). Experimental conditions and display identical to those in Figs. 1 and 2.

Direct or Indirect Effects on Slow Inactivation?

Our results can be interpreted as a direct effect of D4/S4 modification on the slow inactivation mechanism. We will examine two other possibilities here. The first is that MTSES modification of D4/S4 affects other gates that are coupled to the process of slow inactivation. The second is that this modification has no effect, even indirectly, on slow inactivation. Rather, it creates a novel gating process that resembles slow inactivation.

The data of Figs. 1–5 argue against the possibility that the use-dependent current reduction seen with R3C-SES is secondary to effects on fast inactivation, because MTSET has much greater effects on the kinetics of fast inactivation of R3C than MTSES within the hyperpolarized voltage range studied here. Nevertheless, MTSET fails to cause use-dependent current reduction and has little effect on the kinetics of slow inactivation. Another reason to exclude an effect secondary to those on fast inactivation is that residues in the middle of D4/S4 play the largest role in the process of slow inactivation (Fig. 7), whereas mutations at the extracellular end of D4/S4 have the greatest effects on fast inactivation (Yang et al., 1996; Sheets et al., 1999).

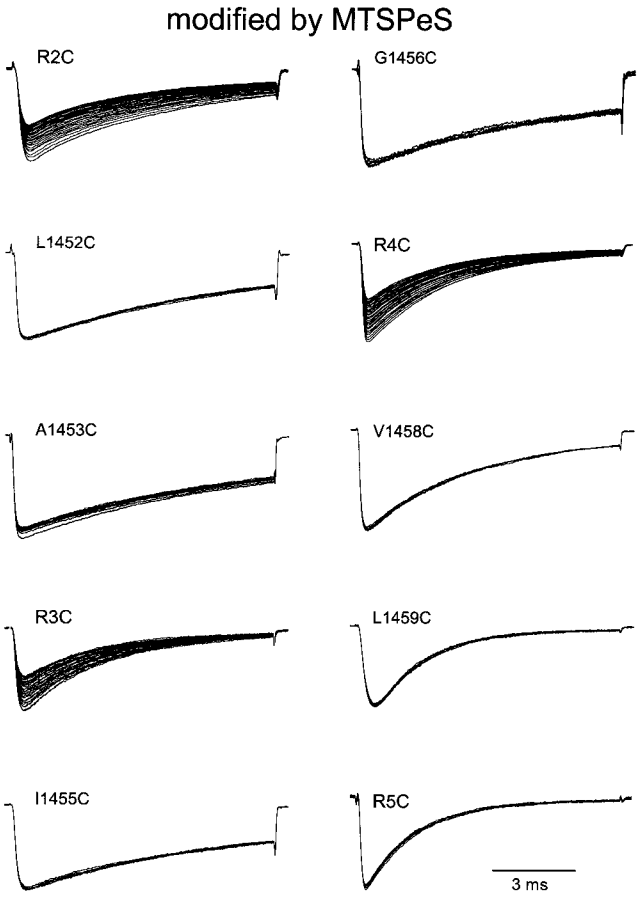

Figure 10. Use dependence after modification by MTSPeS. Data shown for the 10 residues inclusive between R2C and R5C. Experimental conditions and display are identical to those in Fig. 2.

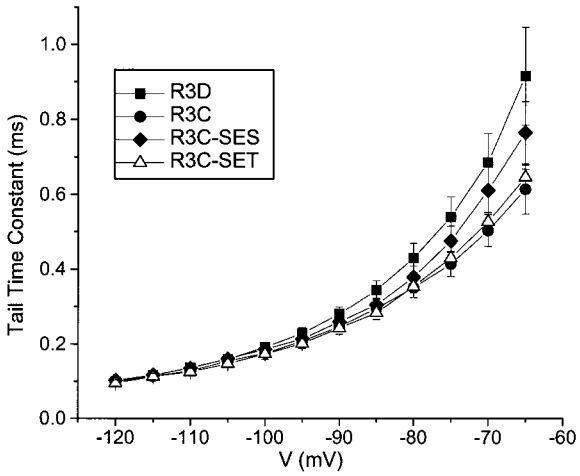

Figure 11. Deactivation kinetics. Tail currents at 12°C were fit by single exponentials with the indicated time constants (n = 3–4 cells).

To examine whether MTSET and MTSES produce distinguishable effects on activation gating of R3C, we examined deactivation kinetics of tail currents. This measurement obviates the difficulty of measuring activation at a depolarized voltage, where the kinetics could be contaminated by effects of cysteine modification on fast inactivation. Furthermore, some mutations of D4/S4 are known to affect deactivation kinetics (Ji et al., 1996; Groome et al., 1999), showing that this S4 segment is likely to be an activation voltage sensor. Tail currents at 12°C were well fit by single exponential relaxations (data not shown). The time constants of R3C tail currents are not affected by either MTSET or MTSES modification at voltages more hyperpolarized than −85 mV (Fig. 11). The mutant R3D also has no effect on tail current kinetics within this voltage range (Fig. 11). The divergence of tail current kinetics at more depolarized voltages is a likely consequence of the effects of altered inactivation of open channels (Aldrich et al., 1983; Vandenberg and Horn, 1984). Thus, deactivation is apparently unperturbed by these modifications of the residue at position 1454. Although deactivation represents only part of the activation pathway, these results support the idea that the effects of MTSES on slow inactivation of the R3C mutant are not secondary to effects on either fast inactivation or activation gating.

Finally, we address the possibility that MTSES modification of R3C creates a new nonconducting state that resembles a slow-inactivated state, rather than producing a direct effect on the native mechanism of slow inactivation. To distinguish these two alternatives, we made use of a pore mutation in domain 1, W408A, in the human skeletal muscle sodium channel that we use in this study. The homologous tryptophan-to-alanine mutation inhibits slow inactivation in sodium channels of rat skeletal muscle (Kambouris et al., 1998). We made the double mutant W408A/R3C and tested whether MTSES produces its typical use-dependent current reduction. If the use dependence is inhibited by the W408A mutation, it suggests that MTSES modification is acting on the same gating process, namely, native slow inactivation.

First, we verified that W408A inhibits slow inactivation in the human isoform of the sodium channel. A 10-s depolarization to −40 mV followed by a 20-ms recovery interval at −140 mV reduces the peak current in a subsequent test pulse by 69.0 ± 2.6% (n = 5) for unmodified R3C (Fig. 5 B), whereas it reduces the peak current only 23.5 ± 5.6% (n = 4) for unmodified W408A/R3C. These results show that W408A strongly reduces the rate of entry into a slow inactivated state at −40 mV. Now we test whether it also interferes with the consequences of MTSES modification of R3C. Fig. 12 shows that MTSES modification of the double mutant causes a use-dependent current reduction (5 Hz), although the magnitude of the effect is significantly smaller than observed in the presence of the native

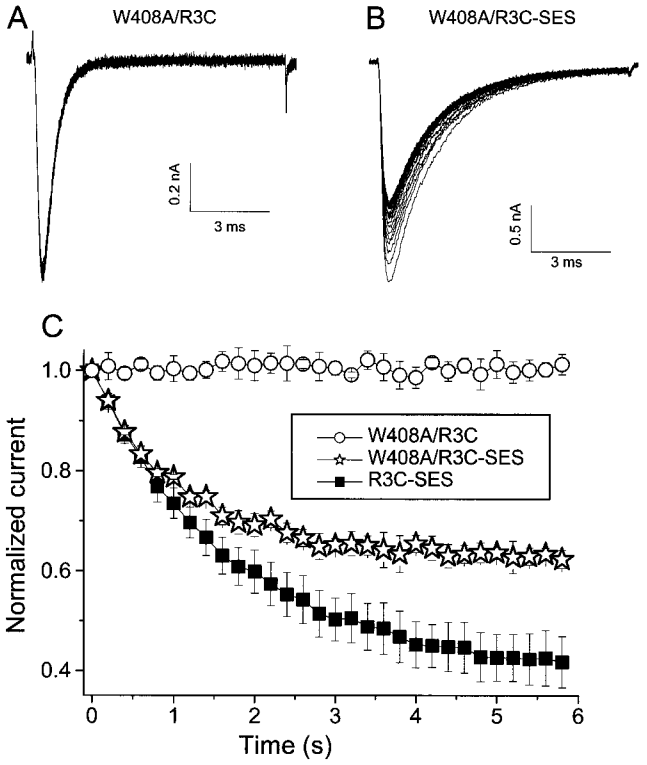

Figure 12. W408A counteracts effects of MTSES on R3C. A and B show 30 superimposed currents using standard 5-Hz protocols (Fig. 2). The normalized reduction of peak currents for the 30 stimuli (n = 3–5 cells) is shown in C. The data for R3C-SES are identical to those in Fig. 3 C.

tryptophan at residue 408 (Fig. 12 C, compare ☆ with ■). Therefore, the W408A mutation partially protects the channel from the effects of MTSES, suggesting that both modifications are acting on the same process, namely, slow inactivation.

DISCUSSION

Our results suggest that the voltage sensor D4/S4 plays a role in slow inactivation. Attachment of S-ethylsulfonate to cysteines introduced near the middle of this transmembrane segment result in an increased propensity to be in a slow-inactivated state. This is a consequence primarily of an increase in the rate of entering this state at depolarized voltages, but there is also a moderate decrease in the rate of leaving this state at hyperpolarized voltages.

What change of molecular structure causes the alteration of slow inactivation by MTSES modification? Clearly, it is not the simple consequence of oxidizing the cysteine sidechain, because MTSET does not produce the same effects (Figs. 2, 4, 5, and 7). Nor is it the negative charge attached to a transmembrane segment that usually contains only cationic or neutral residues, because mutation of the positively charged arginine at position 1454 to either glutamate (R3E) or aspartate (R3D) cannot reproduce this effect of MTSES on R3C (Fig. 9). Furthermore, attachment to R3C of an adduct containing a negatively charged carboxylate group fails to have the effects of MTSES modification on this residue (data not shown). Moreover, the effects on slow inactivation cannot be explained by the fact that MTSES modification increases the bulkiness of the sidechain of D4/S4 residues, because modification of R3C by the larger MTSET does not produce this effect, nor does modification by the much larger reagent tetramethylrhodamine maleimide (data not shown).

We speculate that the sulfonate moiety of the −SES adduct can reach a critical site in the hydrophobic region (the "gating pore") surrounding D4/S4. The principal evidence for this possibility derives from the experiments using MTSPeS, which has a longer linker than MTSES between methanethiosulfonate and the charged sulfonate. MTSPeS has similar effects as MTSES, but it also causes use dependence in R2C, an effect not observed when R2C is modified by the shorter-chained MTSES (Figs. 7 and 10). This suggests that the longer tether allows the sulfonate to reach a site that is intimately involved with slow inactivation. This site is likely to be rather centrally located between the extracellular and intracellular sides of the membrane (Fig. 7). The hypothesis of a critical site in the vicinity of D4/S4 is further supported by the helical pattern in effects of cysteine modification (Fig. 8). Modification of only one face of D4/S4 can affect slow inactivation. If residues extending completely around D4/S4 had had similar effects, then the movement of the S4 segment itself would have been implicated.

Our results suggest that the modifications of D4/S4 that affect slow inactivation act independently of alterations of either activation (Fig. 11) or fast inactivation (Fig. 2). Because slow inactivation is voltage dependent, and because D4/S4 is a voltage sensor for both activation and fast inactivation, it is tempting to propose that D4/S4 is also one of slow-inactivation's voltage sensors. However, we cannot exclude the possibility that modifications of D4/S4 cause effects on slow inactivation that have nothing to do with the fact that D4/S4 is a voltage sensor. For example, MTSES modification of R3C may affect one or more of the transmembrane segments that surround D4/S4. These transmembrane segments could play a role in slow inactivation independent of voltage sensing. We can only conclude that a region of the protein near the middle of D4/S4 plays a significant role in the process of slow inactivation. It is interesting to note that a disease-linked mutation affecting slow inactivation is found in the middle of the S5 segment of D4 (Bendahhou et al., 1999), suggesting that the central region of the gating pore is where the voltage sensor movement is coupled to the slow-inactivation gates.

We thank Mike O'Leary for insightful comments on the manuscript. Thanks also to Craig Short and Nila Gilanni for technical support with DNA sequencing and mutagenesis.

This study was supported by National Institutes of Health grants AR41691 (R. Horn) and NS32387 (A.L. George) and Deutsche Forschungsgemeinschaft grant Mi 472/5-1 (N. Mitrovic).

Submitted: 10 December 1999
Revised: 28 March 2000
Accepted: 11 April 2000

REFERENCES

Aldrich, R.W., D.P. Corey, and C.F. Stevens. 1983. A reinterpretation of mammalian sodium channel gating based on single channel recording. *Nature.* 306:436–441.

Armstrong, C.M. 1981. Sodium channels and gating currents. *Physiol. Rev.* 61:644–683.

Balser, J.R., H.B. Nuss, N. Chiamvimonvat, M.T. Pérez-García, E. Marban, and G.F. Tomaselli. 1996. External pore-lining residue mediates slow inactivation in μ1 rat skeletal muscle sodium channels. *J. Physiol.* 494:431–442.

Barchi, R.L. 1995. Molecular pathology of the skeletal muscle sodium channel. *Annu. Rev. Physiol.* 57:355–385.

Bendahhou, S., T.R. Cummins, R. Tawil, S.G. Waxman, and L.J. Ptácek. 1999. Activation and inactivation of the voltage-gated sodium channel: role of segment S5 revealed by a novel hyperkalaemic periodic paralysis mutation. *J. Neurosci.* 19:4762–4771.

Bezanilla, F. 2000. The voltage sensor in voltage dependent ion channels. *Physiol. Rev.* 80:555–592.

Cannon, S.C. 1996. Sodium channel defects in myotonia and periodic paralysis. *Annu. Rev. Neurosci.* 19:141–164.

Catterall, W.A. 1986. Molecular properties of voltage-sensitive sodium channels. *Annu. Rev. Biochem.* 55:953–985.

Cha, A., P.C. Ruben, A.L. George, Jr., E. Fujimoto, and F. Bezanilla. 1999. Voltage sensors in domains III and IV, but not I and II, are immobilized by Na^+ channel fast inactivation. *Neuron.* 22:73–87.

Chahine, M., A.L. George, Jr., M. Zhou, S. Ji, W. Sun, R.L. Barchi, and R. Horn. 1994. Sodium channel mutations in paramyotonia congenita uncouple inactivation from activation. *Neuron.* 12:281–294.

Chen, L.-Q., V. Santarelli, R. Horn, and R.G. Kallen. 1996. A unique role for the S4 segment of domain 4 in the inactivation of sodium channels. *J. Gen. Physiol.* 108:549–556.

Cummins, T.R., and F.J. Sigworth. 1996. Impaired slow inactivation in mutant sodium channels. *Biophys. J.* 71:227–236.

Fan, Z., A.L. George, Jr., J.W. Kyle, and J.C. Makielski. 1996. Two human paramyotonia congenita mutations have opposite effects on lidocaine block of Na^+ channels expressed in a mammalian cell line. *J. Physiol.* 496:275–286.

Featherstone, D.E., J.E. Richmond, and P.C. Ruben. 1996. Interaction between fast and slow inactivation in Skm1 sodium channels. *Biophys. J.* 71:3098–3109.

Fleig, A., J.M. Fitch, A.L. Goldin, M.D. Rayner, J.G. Starkus, and P.C. Ruben. 1994. Point mutations in IIS4 alter activation and inactivation of rat brain IIA Na channels in *Xenopus* oocyte macropatches. *Pflügers Arch.* 427:406–413.

French, R.J., and R. Horn. 1983. Sodium channel gating: models, mimics, and modifiers. *Annu. Rev. Biophys. Bioeng.* 12:319–356.

Goldman, L. 1999. On mutations that uncouple sodium channel activation from inactivation. *Biophys. J.* 76:2553–2559.

Groome, J.R., E. Fujimoto, A.L. George, Jr., and P.C. Ruben. 1999. Differential effects of homologous S4 mutations in human skeletal muscle sodium channels on deactivation gating from open and inactivated states. *J. Physiol.* 516:687–698.

Hayward, L.J., R.H. Brown, Jr., and S.C. Cannon. 1997. Slow inactivation differs among mutant Na channels associated with myotonia and periodic paralysis. *Biophys. J.* 72:1204–1219.

Hayward, L.J., G.M. Sandoval, and S.C. Cannon. 1999. Defective slow inactivation of sodium channels contributes to familial periodic paralysis. *Neurology.* 52:1447–1453.

Higuchi, R. 1989. Using PCR to engineer DNA. *In* PCR Technology. H.A. Erlich, editor. Stockton Press, New York, NY. 61–70.

Holmgren, M., P.L. Smith, and G. Yellen. 1997. Trapping of organic blockers by closing of voltage-dependent K^+ channels: evidence for a trap door mechanism of activation gating. *J. Gen. Physiol.* 109:527–535.

Ji, S., A.L. George, R. Horn, and R.L. Barchi. 1995. Sodium channel mutations and disorders of excitation in human skeletal muscle. *In* Ion Channels and Genetic Diseases. D.C. Dawson and R.A. Frizzell, editors. Rockefeller University Press, New York, NY. 61–76.

Ji, S., A.L. George, Jr., R. Horn, and R.L. Barchi. 1996. Paramyotonia congenita mutations reveal different roles for segments S3 and S4 of domain D4 in hSkM1 sodium channel gating. *J. Gen. Physiol.* 107:183–194.

Kambouris, N.G., L.A. Hastings, S. Stepanovic, E. Marban, G.F. Tomaselli, and J.R. Balser. 1998. Mechanistic link between lidocaine block and inactivation probed by outer pore mutations in the rat μ1 skeletal muscle sodium channel. *J. Physiol.* 512:693–705.

Keynes, R.D. 1994. The kinetics of voltage-gated ion channels. *Q. Rev. Biophys.* 27:339–434.

Keynes, R.D., and F. Elinder. 1999. The screw-helical voltage gating of ion channels. *Proc. R. Soc. Lond. B Biol. Sci.* 266:843–852.

Kontis, K.J., and A.L. Goldin. 1997. Sodium channel inactivation is altered by substitution of voltage sensor positive charges. *J. Gen. Physiol.* 110:403–413.

Kühn, F.J.P., and N.G. Greeff. 1999. Movement of voltage sensor S4 in domain 4 is tightly coupled to sodium channel fast inactivation and gating charge immobilization. *J. Gen. Physiol.* 114:167–183.

Lehmann-Horn, F., and K. Jurkat-Rott. 1999. Voltage-gated ion channels and hereditary disease. *Physiol. Rev.* 79:1317–1372.

Liu, Y., M. Holmgren, M.E. Jurman, and G. Yellen. 1997. Gated access to the pore of a voltage-dependent K^+ channel. *Neuron.* 19: 175–184.

Makita, N., P.B. Bennett, Jr., and A.L. George, Jr. 1996. Multiple domains contribute to the distinct inactivation properties of human heart and skeletal muscle Na^+ channels. *Circ. Res.* 78:244–252.

Nuss, H.B., J.R. Balser, D.W. Orias, J.H. Lawrence, G.F. Tomaselli, and E. Marban. 1996. Coupling between fast and slow inactivation revealed by analysis of a point mutation (F1304Q) in μ1 rat skeletal muscle sodium channels. *J. Physiol.* 494.2:411–429.

Patlak, J. 1991. Molecular kinetics of voltage-dependent Na^+ channels. *Physiol. Rev.* 71:1047–1080.

Sheets, M.F., J.W. Kyle, R.G. Kallen, and D.A. Hanck. 1999. The Na channel voltage sensor associated with inactivation is localized to the external charged residues of domain IV, S4. *Biophys. J.* 77: 747–757.

Sigworth, F.J. 1994. Voltage gating of ion channels. *Q. Rev. Biophys.* 27:1–40.

Strichartz, G.R. 1973. The inhibition of sodium current in myelinated nerve by quaternary derivatives of lidocaine. *J. Gen. Physiol.* 62:37–57.

Takahashi, M.P., and S.C. Cannon. 1999. Enhanced slow inactivation by V445M: a sodium channel mutation associated with myotonia. *Biophys. J.* 76:861–868.

Todt, H., S.C. Dudley, Jr., J.W. Kyle, R.J. French, and H.A. Fozzard. 1999. Ultra-slow inactivation in μ1 Na^+ channels is produced by a structural rearrangement of the outer vestibule. *Biophys. J.* 76:

1335–1345.

Townsend, C., and R. Horn. 1997. Effect of alkali metal cations on slow inactivation of cardiac Na^+ channels. *J. Gen. Physiol.* 110:23–33.

Vandenberg, C.A., and R. Horn. 1984. Inactivation viewed through single sodium channels. *J. Gen. Physiol.* 84:535–564.

Vedantham, V., and S.C. Cannon. 1998. Slow inactivation does not affect movement of the fast inactivation gate in voltage-gated Na^+ channels. *J. Gen. Physiol.* 111:83–93.

Vilin, Y.Y., N. Makita, A.L. George, and P.C. Ruben. 1999. Structural determinants of slow inactivation in human cardiac and skeletal muscle sodium channels. *Biophys. J.* 77:1384–1393.

Wang, S.Y., and G.K. Wang. 1997. A mutation in segment I-S6 alters slow inactivation of sodium channels. *Biophys. J.* 72:1633–1640.

West, J.W., D.E. Patton, T. Scheuer, Y. Wang, A.L. Goldin, and W.A. Catterall. 1992. A cluster of hydrophobic amino acid residues required for fast Na^+-channel inactivation. *Proc. Natl. Acad. Sci. USA.* 89:10910–10914.

Yang, N., A.L. George, and R. Horn. 1997. Probing the outer vestibule of a sodium channel voltage sensor. *Biophys. J.* 73:2260–2268.

Yang, N., A.L. George, Jr., and R. Horn. 1996. Molecular basis of charge movement in voltage-gated sodium channels. *Neuron.* 16: 113–122.

Yang, N., and R. Horn. 1995. Evidence for voltage-dependent S4 movement in sodium channels. *Neuron.* 15:213–218.

Yellen, G. 1998. The moving parts of voltage-gated ion channels. *Q. Rev. Biophys.* 31:239–295.